CHEMISTRY OF MATERIALS
Article

Chem. Mater. **2010,** *22,* 2481–2490 2481
DOI:10.1021/cm903125v

Porphyrins Intercalated in Zn/Al and Mg/Al Layered Double Hydroxides: Properties and Structural Arrangement

Eva Káfuňková,[†,§] Christine Taviot-Guého,[‡] Petr Bezdička,[†] Mariana Klementová,[†] Petr Kovář,[⊥] Pavel Kubát,[∥] Jiří Mosinger,[†,§] Miroslav Pospíšil,[⊥] and Kamil Lang*[,†]

[†]*Institute of Inorganic Chemistry, v.v.i., Academy of Sciences of the Czech Republic, 250 68 Řež, Czech Republic,* [‡]*Laboratoire des Materiaux Inorganiques, Universite Blaise Pascal, UMR-CNRS no. 6002, 63177 Aubiere Cedex, France,* [§]*Department of Inorganic Chemistry, Faculty of Science, Charles University in Prague, Hlavova 2030, 128 43 Praha, Czech Republic,* [⊥]*Faculty of Mathematics and Physics, Charles University in Prague, Ke Karlovu 3, 121 16 Praha 2, Czech Republic, and* [∥]*J. Heyrovský Institute of Physical Chemistry, v.v.i., Academy of Sciences of the Czech Republic, Dolejškova 3, 182 23 Praha 8, Czech Republic*

Received October 9, 2009. Revised Manuscript Received February 7, 2010

The arrangement of porphyrin molecules in the interlayer space of layered double hydroxides (LDH) has been studied by a combination of experimental techniques and molecular dynamics simulations. Intercalation of 5,10,15,20-tetrakis(4-sulfonatophenyl)porphyrins (TPPS) into Zn_RAl and Mg_RAl LDH hosts led to a gallery height of about 15.5 Å that is comparable with the size of the porphyrin molecules. The porphyrin sulfonate groups are located at about 4 Å from the center of the hydroxide layers that is consistent with hydrogen bonding interactions between the sulfonate groups and OH groups of the layers. The aromatic ring system in the middle of the gallery is rather disordered. A large number of in-plane diffraction lines suggests that the rigidity of the porphyrin framework has a beneficial effect on the layer ordering. Molecular dynamics simulations are in agreement with the experimental results showing that the interlayer space is filled with nearly parallel porphyrin units with a slightly inclined orientation of the porphyrin planes with respect to the normal of the hydroxide layers. The photophysical experiments proved that TPPS in Mg_2Al LDH hosts produce $O_2(^1\Delta_g)$ with long effective lifetimes. The LDH hybrids based on intercalated porphyrin sensitizers are suggested as new photofunctional materials.

Introduction

The prospect of obtaining novel materials gave impetus to studies of molecules immobilized in clays, layered double hydroxides (LDH), zeolites, or sol−gel derived matrices.[1−7] Layered solids are materials that can be functionalized by intercalation of active molecules with specific properties. In this case, layered structures act as hosts with a two-dimensional expandable interlayer space for the placement and organization of guest molecules. The intercalated solids not only provide an easy-to-apply transport material, but mostly increase chemical, photochemical, and thermal stability of guests including the control of their release during applications.[8,9] The constrained geometry, enforced by host−guest noncovalent interactions, is reflected in physicochemical and photophysical properties of guest molecules.[10]

LDH are nanostructured materials of the general formula $[M_{1-x}^{2+}M_x^{3+}(OH)_2]A_{x/m}^{m-}\cdot nH_2O$, abbreviated hereafter as $M_R^{2+}M^{3+}$−A, where M^{2+} and M^{3+} are divalent and trivalent cations, respectively, A is an anion of valence m and $R = (1 - x)/x$ is the M^{2+}/M^{3+} molar ratio. Their lamellar structure consists of brucite-like layers of positive charge counterbalanced by anionic species in the interlayer space together with water molecules.[11,12] LDH have attracted much attention owing to their ability to intercalate a wide variety of anions, either organic or inorganic. As a consequence, LDH have found potential applications in catalysis,[13] wastewater treatment,[14−16] electrochemical sensors,[17] or as fillers in polymers.[18] Furthermore, LDH are environmentally friendly, biocompatible

*Author to whom correspondence should be addressed. E-mail: lang@iic.cas.cz.

(1) Rives, V.; Ulibarri, M. A. *Coord. Chem. Rev.* **1999**, *181*, 61.
(2) Evans, D. G.; Duan, X. *Chem. Commun.* **2006**, 485.
(3) Ogawa, M.; Kuroda, K. *Chem. Rev.* **1995**, *95*, 399.
(4) Choy, J.-H.; Choi, S.-J.; Oh, J.-M.; Park, T. *Appl. Clay Sci.* **2007**, *36*, 122.
(5) Costantino, U.; Ambrogi, V.; Nocchetti, M.; Perioli, L. *Microporous Mesoporous Mater.* **2008**, *107*, 149.
(6) Takagi, S.; Eguchi, M.; Tryk, D. A.; Inoue, H. *J. Photochem. Photobiol. C* **2006**, *7*, 104.
(7) Wang, S.; Gao, R.; Zhou, F.; Selke, M. *J. Mater. Chem.* **2004**, *14*, 487.
(8) Laguna, H.; Loera, S.; Ibarra, I. A.; Lima, E.; Vera, M. A.; Lara, V. *Microporous Mesoporous Mater.* **2007**, *98*, 234.
(9) Wei, M.; Pu, M.; Guo, J.; Han, J.; Li, F.; He, J.; Evans, D. G.; Duan, X. *Chem. Mater.* **2008**, *20*, 5169.
(10) Lang, K.; Mosinger, J.; Wagnerová, D. M. *Coord. Chem. Rev.* **2004**, *248*, 321.
(11) Leroux, F.; Taviot-Guého, C. *J. Mater. Chem.* **2005**, *15*, 3628.
(12) Evans, D. G.; Slade, R. C. T. *Layered Double Hydroxides, Structural Bonding*; Duan, X., Evans, D. G., Eds.; Springer-Verlag: Berlin, Heidelberg, 2006; Vol. *119*; p 1−87.
(13) An, Z.; Zhang, W. H.; Shi, H. M.; He, J. *J. Catal.* **2006**, *241*, 319.
(14) Kovanda, F.; Kovácsová, E.; Koloušek, D. *Collect. Czech. Chem. Commun.* **1999**, *64*, 1517.

Published on Web 03/12/2010

materials with possible use as drug stabilizers and carriers.[19,20] The important features are the flexibility of the two-dimensional interlayer space and the variable charge density of the hydroxide layers (x usually lies between 0.20 and 0.35) allowing the incorporation of variable amounts of bulky guest molecules[21,22] including porphyrins and phthalocyanines.[1,23−27]

Porphyrins and related macrocycles are photosensitizers with rich fluorescence properties and the ability to produce singlet oxygen, $O_2(^1\Delta_g)$.[10] The photosensitized production of $O_2(^1\Delta_g)$ is based on excitation of a photosensitizer to the triplet states and energy transfer of this energy to the ground electronic state of oxygen that is excited to the lowest singlet state, $O_2(^1\Delta_g)$. The oxidative potential of $O_2(^1\Delta_g)$ can be exploited in chemical syntheses, photodynamic treatment of cancer, and disinfection. Planar porphyrin molecules tend to form stacked aggregates, in which absorbed excitation energy is dissipated through decay channels competing with desired photoinitiated reactions.[10,28] The aggregation can be eliminated by the immobilization of the individual molecules in inorganic hosts of ordered structures such as LDH or layered silicates.[3,6,11,24] In addition, the advantages are well-defined microscopic structures of the host matrices, specific organization, variability, and enhanced stability of the photoactive molecules. Recently, we have described the structural and photophysical properties of porphyrin−LDH hybrids prepared by ion exchange and shown that the porphyrin triplet states interact with oxygen molecules in the LDH interlayer to form $O_2(^1\Delta_g)$.[29] These hybrids can serve as handy sources of $O_2(^1\Delta_g)$ and in the form of films they are suitable, e.g., for the construction of bactericidal surfaces.[30]

Molecular dynamics simulations in combination with powder X-ray diffraction (XRD) provide new information on the structural features, dynamics, and arrangement of the interlayer water and anions, the properties mostly not available by direct measurements.[12,31,32] We recently modeled Mg_2Al LDH with 5,10,15,20-tetrakis(4-sulfonatophenyl)porphyrin (TPPS) in the interlayer and compared the measured XRD patterns of the sample prepared by anion exchange with simulated patterns.[33] The porphyrin units are horizontally shifted to each other, disordered, and inclined with respect to the hydroxide layers.

In the present work, we have investigated the intercalation of anionic TPPS and Zn(II)-5,10,15,20-tetrakis(4-sulfonatophenyl)porphyrin (ZnTPPS) into Zn_RAl and Mg_RAl LDH by the coprecipitation method. In general, Zn_RAl LDH hybrids exhibit higher crystallinity than corresponding hybrids based on Mg_RAl LDH. The gain in crystallinity was accompanied with the stabilization of a Zn^{2+}/Al^{3+} ratio equal to 2, and with the appearance of many in-plane diffraction lines in XRD that allowed us to propose, for the first time, a structural model of the interlayer space of Zn_RAl LDH hosts. Molecular dynamics simulations and XRD refinements indicate an inclined orientation of the porphyrin planes with respect to the hydroxide layers. The formation of $O_2(^1\Delta_g)$ by porphyrin−LDH hybrids is also presented.

Materials and Methods

Preparation. The tetrasodium salt of TPPS (Aldrich, Germany), $Al(NO_3)_3\cdot 9H_2O$, $AlCl_3\cdot 6H_2O$, $Zn(NO_3)_2\cdot 6H_2O$, $ZnCl_2\cdot 6H_2O$, $Mg(NO_3)_2\cdot 6H_2O$, $MgCl_2\cdot 6H_2O$, and NaOH (all by Acros Organics, France) were used as purchased. Deionized and decarbonated water was used throughout all experiments.

The LDH samples were prepared at constant pH using a coprecipitation technique adjusted to small quantities.[24,34] A solution of Zn^{2+} and Al^{3+} (3 mL, 0.2 M) in a variable molar ratio ($R = Zn^{2+}/Al^{3+} = 2-4$) was slowly added at a rate of 0.01 mL/min to 10 mL of an aqueous TPPS solution. TPPS was in a 2-fold molar excess over the stoichiometry. In some experiments, ZnTPPS obtained by stirring TPPS with an equimolar amount of Zn^{2+} for 1 h, was used instead of pure TPPS. The pH value was maintained constant at pH 7.5 for $R = 2$ and 3 and at pH 8.0 for $R = 4$ by the simultaneous addition of 0.4 M NaOH. Coprecipitation was carried out under vigorous stirring in a nitrogen atmosphere at room temperature in order to avoid dissolution of atmospheric CO_2 and subsequent contamination by carbonate anions. The addition of NaOH was completed after 5 h, and the resulting violet precipitate was aged for 24 h under stirring. The product was centrifuged, washed three times with water, and finally dried in air at room temperature. All

(15) Wang, Y. F.; Gao, H. Z. *J. Colloid Interface Sci.* **2006**, *301*, 19.
(16) Lakraimi, M.; Legrouri, A.; Barroug, A.; de Roy, A.; Besse, J. P. *Mater. Res. Bull.* **2006**, *41*, 1763.
(17) Mousty, C. *Appl. Clay Sci.* **2004**, *27*, 159.
(18) Taviot-Guého, C.; Leroux, F. *Layered Double Hydroxides, Structural Bonding*; Duan, X.; Evans, D. G., Eds.; Springer-Verlag: Berlin, Heidelberg, 2006; Vol. 119, p 121−159.
(19) (a) Khan, A. I.; O'Hare, D. *J. Mater. Chem.* **2002**, *12*, 3191. (b) Khan, A. I.; Ragavan, A.; Fong, B.; Markland, C.; O'Brien, M.; Dunbar, T. G.; Williams, G. R.; O'Hare, D. *Ind. Eng. Chem. Res.* **2009**, *48*, 10196.
(20) Del Hoyo, C. *Appl. Clay Sci.* **2007**, *36*, 103.
(21) Latterini, L.; Nocchetti, M.; Aloisi, G. G.; Costantino, U.; Elisei, F. *Inorg. Chim. Acta* **2007**, *360*, 728.
(22) Marangoni, R.; Taviot-Guého, C.; Illaik, A.; Wypych, F.; Leroux, F. *J. Colloid Interface Sci.* **2008**, *326*, 366.
(23) Ukrainczyk, L.; Chibwe, M.; Pinnavaia, T. J.; Boyd, S. A. *J. Phys. Chem.* **1994**, *98*, 2668.
(24) Bonnet, S.; Forano, C.; de Roy, A.; Besse, J. P.; Maillard, P.; Momenteau, M. *Chem. Mater.* **1996**, *8*, 1962.
(25) Wark, M. Porphyrins and Phthalocyanines in Inorganic Host Materials. *The Porphyrin Handbook*; Kadish, K. M., Smith, K. M., Guillard, R., Eds.; Elsevier Science: New York, 2003; Vol. *17*.
(26) Barbosa, C. A. S.; Ferreira, A. M. D. C.; Constantino, V. R. L. *Eur. J. Inorg. Chem.* **2005**, 1577.
(27) Halma, M.; de Freitas Castro, K. A. D; Taviot-Guého, C.; Prévot, V.; Forano, C.; Wypych, F.; Nakagaki, S. *J. Catal.* **2008**, *257*, 233.
(28) Sandanayaka, A. S. D.; Araki, Y.; Wada, T.; Hasobe, T. *J. Phys. Chem. C* **2008**, *112*, 19209.
(29) Lang, K.; Bezdička, P.; Bourdelande, J. L.; Hernando, J.; Jirka, I.; Káfuňková, E.; Kovanda, F.; Kubát, P.; Mosinger, J.; Wagnerová, D. M. *Chem. Mater.* **2007**, *19*, 3822.
(30) Lang, K.; Kubát, P.; Mosinger, J.; Bujdák, J.; Hof, M.; Janda, P.; Sýkora, J.; Iyi, N. *Phys. Chem. Chem. Phys.* **2008**, *10*, 4429.
(31) (a) Newman, S. P; Cristina, T. D.; Coveney, P. V.; Jones, W. *Langmuir* **2002**, *18*, 2933. (b) Yan, D.; Lu, J.; Wei, M.; Li, H.; Ma, J.; Li, F.; Evans, D. G.; Duan, X. *J. Phys. Chem. A* **2008**, *112*, 7671.
(32) (a) Lombardo, G. M.; Pappalardo, G. C.; Punzo, F.; Costantino, F.; Costantino, U.; Sisani, M. *Eur. J. Inorg. Chem.* **2005**, 5026. (b) Lombardo, G. M.; Pappalardo, G. C.; Costantino, F.; Costantino, U.; Sisani, M. *Chem. Mater.* **2008**, *20*, 5585.
(33) Kovář, P.; Pospíšil, M.; Káfuňková, E.; Lang, K.; Kovanda, F. *J. Mol. Model.* **2010**, *16*, 223.
(34) Miyata, S. *Clays Clay Miner.* **1975**, *23*, 369.

samples were then submitted to a hydrothermal treatment. Typically, about 20 mg of the solids was suspended in 25 mL of water in a 30 mL Teflon inner vessel in a stainless autoclave and treated at 120 °C for 72 h under autogenous pressure. Mg_RAl LDH hybrids were synthesized similarly.

The samples were labeled, e.g., as Zn_2Al-TPPS, Zn_2Al-(Zn)TPPS^H, and Zn_2Al-ZnTPPS where the molar ratio M^{2+}/Al^{3+} (R) used in the synthesis is given by subscript, the superscript H stands for hydrothermally treated samples, and the porphyrin used for the synthesis is expressed by TPPS or ZnTPPS. The fact that originally used TPPS was metalated to ZnTPPS during the hydrothermal treatment is indicated by (Zn). Zn_RAl-Cl LDH intercalated with chloride anions is used here as a reference.

Characterization Techniques. Powder X-ray diffraction (XRD) (see the Supporting Information) was performed on a PANalytical X'Pert PRO X-ray diffractometer in the Bragg−Brentano geometry. The sample Zn_2Al-ZnTPPS^H of high crystallinity was also analyzed in the Debye−Scherrer geometry equipped with a capillary sample holder and a hybrid mirror monochromator ($CuK\alpha_1$, λ = 1.540598 Å). In-situ high-temperature measurements were performed using a high-temperature Anton PAAR HTK-16 chamber.

The diffuse reflectance UV−visible spectra were acquired on a Perkin-Elmer Lambda 35 spectrometer equipped with a Labsphere RSA-PE-20 integration sphere. Thermogravimetric analyses (TG-DTA) were carried out on a Setaram SETSYS Evolution instrument in air. The gas emission analysis was performed using a Setaram SETSYS Evolution-16-MS coupled with a mass spectroscopy system. High-resolution transmission electron microscopy (HRTEM) was carried out on a JEOL JEM 3010 microscope operated at 300 kV (LaB_6 cathode, point resolution 1.7 Å). The time-resolved near-infrared luminescence of $O_2(^1\Delta_g)$ at 1270 nm was monitored using a Ge diode detector upon laser excitation by a Lambda Physik FL 3002 dye laser (λ_{exc} = 425 nm, incident energy ~ 1 mJ/pulse). The detailed description of all methods is given in the Supporting Information.

Molecular Modeling. Molecular mechanics and classical molecular dynamics[35] were carried out in the Cerius and Materials Studio modeling environment (see the Supporting Information).[36] The structure of ZnTPPS was optimized by the quantum-chemistry computational program Turbomole v5.9.[37] $Zn_2Al-LDH$ is created as a trilayered structure with a trigonal cell in hexagonal axes.[33] The space group is $R\bar{3}m$, and the initial experimental cell parameters used were $a = b$ = 3.064 Å. The basal spacing d_{003} was 23.05 Å. A layer $[Zn_{64}Al_{32}(OH)_{192}]^{32+}$ was created by the linking of 96 individual cells to give the lattice parameters of A = 49.024 Å and B = 18.384 Å, with Al^{3+} cations distributed in the layers on the condition that the location of Al^{3+} in neighboring octahedra is excluded.[38] The total composition was $[Zn_{192}Al_{96}(OH)_{576}](ZnTPPS)_{24}\cdot 192\,H_2O$ with the space group set to P1. Charges were calculated by the Qeq method.[39] The initial models were minimized in the Universal force field, the electrostatic energy was calculated by the Ewald summation method,[40] and the van der Waals energy was calculated by the Lennard-Jones potential.[41] The dynamics simulations were carried out in an NVT statistical ensemble at 300 K. One dynamic step was 0.001 ps, and dynamics of 200 ps were carried out.

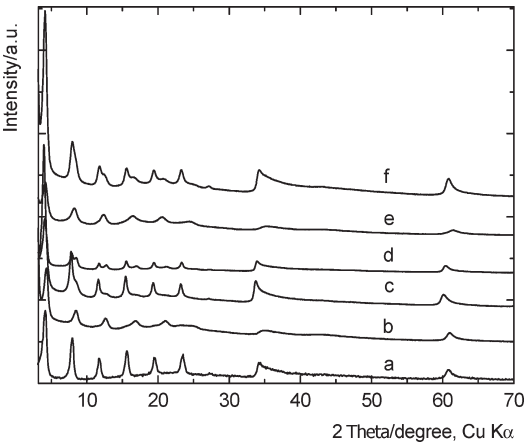

Figure 1. Powder XRD patterns of samples before hydrothermal treatment: $Zn_2Al-ZnTPPS$ (a), $Mg_4Al-TPPS$ (b), $Zn_4Al-TPPS$ (c), $Zn_3Al-TPPS$ (d), $Mg_2Al-TPPS$ (e), and $Zn_2Al-TPPS$ (f).

Results and Discussion

Characterization of LDH Intercalated with Porphyrins. The coprecipitation method facilitates the effective intercalation of bulky porphyrin anions to compensate for the positive charge of the layers. Furthermore, this method often viewed as a self-assembly process should permit an adjustment of the M^{2+}/M^{3+} ratio, i.e., to control the layer charge density and make it coincide with the charge *per* unit area for the intercalated anion. The composition based on Zn^{2+} and Al^{3+} is advantageous because Zn_RAl LDH hosts usually have higher crystallinity than Mg_RAl LDH. Here, we present the properties of both Zn_RAl and Mg_RAl LDH hybrids.

The XRD patterns of as-prepared samples were recorded in the Bragg−Brentano geometry and were all indexed in the rhombohedral space group $R\bar{3}m$, typical for LDH-based systems (Figure 1). A splitting of 003n basal lines of Zn_RAl LDH indicates two phases with close interlayer distances that are both consistent with the intercalation of the porphyrin molecules. The cell parameters, shown in Table 1, were obtained from the peak profile analysis, and it should be noted that the spherical harmonics correction for an anisotropic peak broadening[42] due to size effects was essential to reach a good fit. The molar ratios R_{calc} were derived from a relationship between the cell parameter a and the M^{2+}/M^{3+} molar ratio established for the Zn_RAl and Mg_RAl LDH series.[43] Both calculated, R_{calc}, and experimental, R_{exp}, values are comparable and in agreement with the initial molar ratios used for the synthesis (Table 1). The molar ratio

(35) Comba, P; Hambley, T. W. *Molecular Modeling of Inorganic Compounds*; VCH Verlagsgesselschaft mbH: Weinheim, 1995.
(36) Accelrys Software Inc. *Materials Studio Modeling Environment*; release 4.3 documentation, Accelrys Software Inc.: San Diego, 2003.
(37) Ahlrichs, R.; Bär, M.; Häser, M.; Horn, H.; Kölmel, C. *Chem. Phys. Lett.* **1989**, *162*, 165.
(38) Sideris, P. J.; Nielsen, U. G.; Gan, Z.; Grey, C. P. *Science* **2008**, *321*, 113.
(39) Rappe, A. K; Goddard, W. A.III *J. Phys. Chem.* **1991**, *95*, 3358.
(40) Karasawa, N; Goddard, W. A.III *J. Phys. Chem.* **1989**, *93*, 7320.
(41) Lennard-Jones, J. E. *Proc. R. Soc. London, Ser. A* **1925**, *109*, 584.
(42) Rodríguez-Carvajal, J. *Newslett. Powder Diff. Comm. Int. Union Crystallogr.* **2001**, *26*, 12.
(43) Leroux, F.; Adachi-Pagano, M.; Intissar, M.; Chauvière, S.; Forano, C.; Besse, J. P. *J. Mater. Chem.* **2001**, *11*, 105.

Table 1. Refined Cell Parameters of Porphyrin−LDH Hybrids and the Molar M^{2+}/M^{3+} Ratios Obtained from XRD (R_{calc}) and Elemental Analysis (R_{exp})

samples	a/Å	c/Å	d_{003}/Å	R_{calc}	R_{exp}
Mg_2Al−TPPS	3.0300(3)	65.093(9)	21.70	1.5	
Mg_2Al−$TPPS^H$	3.0351(2)	69.105(5)	23.03	1.8	1.73
Zn_2Al−TPPS	3.0548(2)	68.856(3)	22.95	1.8	1.94
	3.0548(2)	64.332(9)	21.44		
Zn_2Al−(Zn)$TPPS^H$	3.0568(4)	68.702(9)	22.90	1.7	1.90
Zn_2Al−ZnTPPS	3.0621(2)	69.215(7)	23.07	1.8	
Zn_2Al−$ZnTPPS^H$	3.0625(3)	69.090(1)	23.03	1.8	1.91
Zn_4Al−TPPS	3.0859(3)	68.909(9)	22.97	4.1	3.60
	3.0859(3)	63.740(3)	21.25		
Zn_4Al−(Zn)$TPPS^H$	3.0667(2)	69.047(4)	23.01	2.1	3.05

sulfur/Al^{3+} suggests that over 80% of hydroxide positive charges were compensated by the sulfonated groups of the porphyrin molecule. An explanation for the origin of the two interlayer distances can be deduced from the absorption spectra and thermal behavior. The absorption spectrum of pure TPPS displays the Soret band at 412 nm and four Q bands at 516, 550, 590, and 647 nm, while ZnTPPS shows the intensive Soret band at 424 nm and only two Q bands peaking at 561 and 603 nm due to the increase of the porphyrin symmetry (Figure 2). The spectra of Zn_RAl−TPPS differ from those of pure TPPS showing a red-shifted Soret band of 423 nm and more intensive absorptions at 560 and 600 nm, while the spectra of Mg_RAl−TPPS and TPPS have the same features. This documents a partial metalation of TPPS by Zn^{2+} during the Zn_RAl LDH synthesis. This is further corroborated by Zn_2Al−ZnTPPS, prepared using ZnTPPS, whose spectrum equals that of pure ZnTPPS (Figure 2) and the XRD patterns are not split as in the case of Zn_2Al−TPPS (Figure 1). Evidently, Mg_2Al−TPPS is characterized by a single basal spacing of 21.70 Å, while two phases containing either TPPS or ZnTPPS within the Zn_2Al LDH interlayer space result in two different basal spacings of 21.44 and 22.95 Å, respectively.

Although the absorption spectra clearly show the presence of both TPPS and ZnTPPS in Zn_RAl−TPPS, one must check whether the variations of the interlayer water content might also contribute to the two distances observed by XRD. Hence, the thermal behavior of Zn_4Al−TPPS

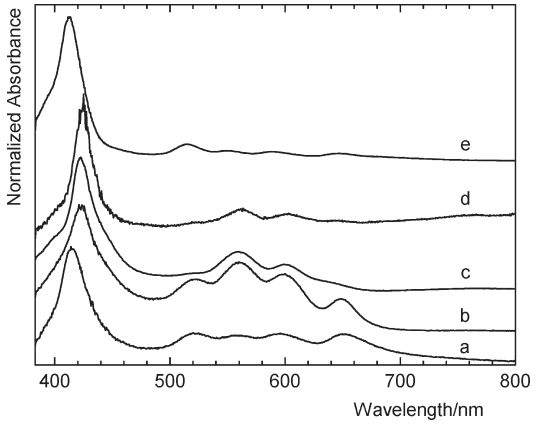

Figure 2. Normalized diffuse reflectance spectra before hydrothermal treatment: Mg_2Al−TPPS (a), Zn_2Al−TPPS (b), and Zn_2Al−ZnTPPS (c) compared with ZnTPPS (d) and TPPS (e).

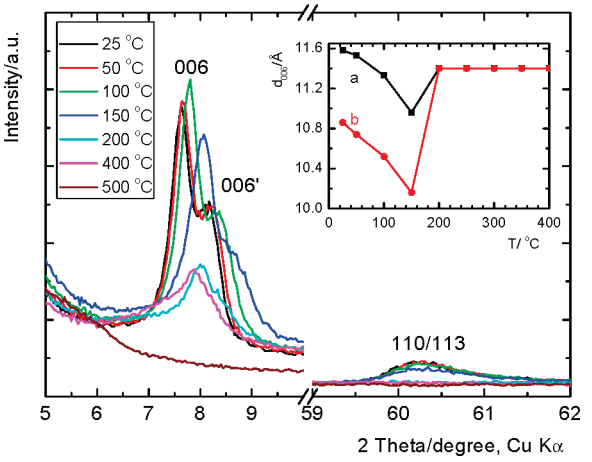

Figure 3. In-situ high-temperature XRD patterns of Zn_4Al-TPPS. The inset shows the relationship between the d_{006} (a) and $d_{006'}$ (b) basal spacings and temperature.

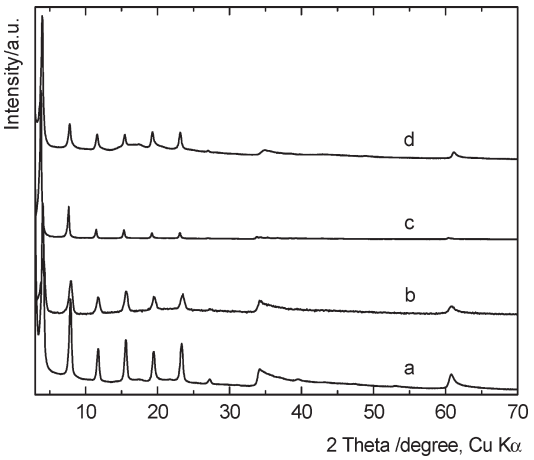

Figure 4. Powder XRD patterns of Zn_2Al−(Zn)$TPPS^H$ (a), Zn_2Al−ZnTPPS (b), Zn_2Al−$ZnTPPS^H$ (c), and Mg_2Al−$TPPS^H$ (d).

was examined by *in situ* high-temperature XRD (Figure 3). A gradual shift of the 006 double line toward higher 2θ values after increasing temperature from 50 to 150 °C indicates a decrease of the interlayer distance due to the removal of interlayer water. This was also confirmed by mass spectroscopy during thermogravimetric analysis (see below). The intensity of the 006 lines reaches a maximum at 100 °C suggesting a maximal ordering of the interlayer at this temperature. At 200 °C, dehydroxylation of the hydroxide layers is evidenced by the collapse and disappearance of the 006 and 110/113 lines, respectively. The fact that the 006 double line does not merge into a single line, even at 150 °C, supports the existence of two distinct phases that differ in the nature of intercalated porphyrin. Indeed, if these two basal lines were due to the different interlayer water content, we would have expected the two peaks to fuse into a single peak during interlayer dehydration.

The hydrothermal treatment causes a net increase of crystallinity of all samples (Table 1, Figure 4). The disappearance of the two-phase XRD patterns (Figures 1 and 4) and corresponding absorption spectra document that originally intercalated TPPS in Zn_RAl

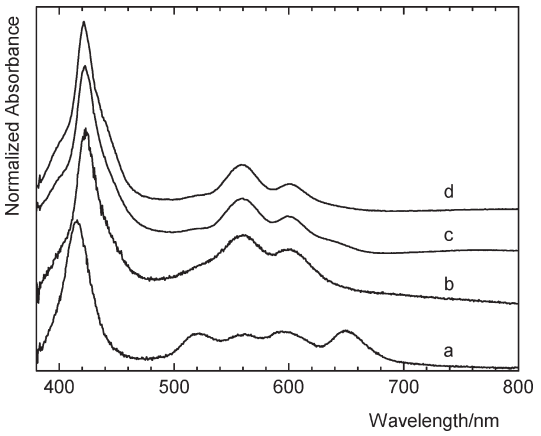

Figure 5. Normalized diffuse reflectance spectra of $Mg_2Al-TPPS^H$ (a), $Zn_2Al-(Zn)TPPS^H$ (b), and $Zn_2Al-ZnTPPS$ (c) compared with $Zn_2Al-ZnTPPS^H$ (d).

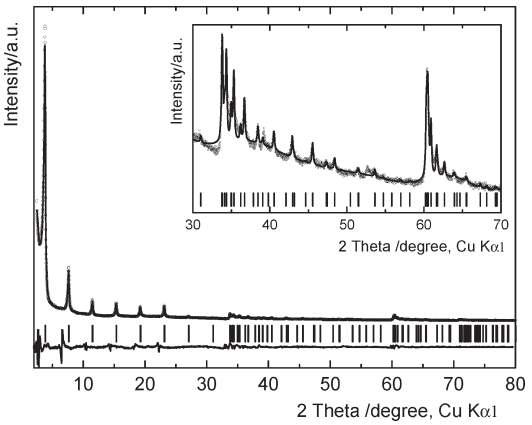

Figure 6. Profile analysis of the XRD pattern of $Zn_2Al-ZnTPPS^H$ recorded in the Debye−Scherrer geometry: experimental X-ray diffraction (circles), calculated (line), Bragg reflections (ticks), and difference profiles. Refined unit cell parameters: $a = 3.0604(6)$ Å and $c = 69.01(1)$ Å. $R_{Bragg} = 0.08\%$. (inset) Extended region $30-70°/2\theta$.

LDH is completely metalated to ZnTPPS, while intercalated TPPS in Mg_RAl LDH remains unchanged (Figure 5). It is worth noting that TPPS metalation is not unexpected due to the high affinity of TPPS toward free Zn^{2+} in solution. The XRD patterns of $Zn_3Al-(Zn)TPPS^H$ and $Zn_4Al-(Zn)TPPS^H$ newly show the diffraction lines of ZnO that is accompanied by a decrease of the Zn^{2+}/Al^{3+} ratio (R_{calc}) within the hydroxide layers to 2 as deduced from the decrease of the cell parameter a (Table 1). It can be attributed to a dissolution/decomposition of Zn-based LDH during the hydrothermal treatment in conjunction with the low octahedral crystal field stabilization energy of Zn^{2+} ions.[44] In contrast, the metal ratio in Zn_2Al LDH host remains unchanged with no signs of the ZnO presence. The stability of Zn_2Al LDH under specific hydrothermal conditions indicates that the most energetically favorable host−guest charge and structure alignment are reached at this molar ratio.

The absorption spectra (Figure 5) and XRD patterns of $Zn_2Al-ZnTPPS$ and $Zn_2Al-ZnTPPS^H$ (Figures 4 and 6) document the stability of ZnTPPS in the interlayer space and very high crystallinity after the hydrothermal treatment. This is indicated by not only the very narrow 003n basal lines, but also by the appearance of many 10n and 01n in-plane lines at high 2θ angle values. One must say that the observation of the in-plane reflections is quite rare in LDH. The high crystallinity of $Zn_2Al-ZnTPPS^H$ allowed us to extract additional information on the intercalate structure (see below).

Thermal Behavior. The amount of physisorbed and interlayer/structural water molecules can be determined using thermogravimetric analyses (Table 2). The TG-DTA curves, describing the general thermal behavior of hybrids, have similar features (Supporting Information Figure S1). The amount of physisorbed water was determined by evacuating the samples at 50 °C for 5 h. The thermal processes are characterized by three weight loss steps. Depending on sample crystallinity, all these thermal events are either well-separated or superimposed phenomena. The loss between 50 and 150 °C, accompanied by a decrease of the interlayer spacing (Figure 3), is attributed to the removal of interlayer water molecules. The results show that 40−75% of total water belongs to physisorbed water molecules. The number of intercalated water molecules is close to that reported for LDH, i.e., about two water molecules per Zn_2Al formula unit. In the case of Mg_2Al LDH, the obtained number is less accurate because of less defined weight losses related to their lower crystallinity. The second step (150−400 °C) involves two simultaneous processes, dehydroxylation of the brucite-like layers, and decomposition of interlayer anions, while the third step above 400 °C is a consequence of decomposition and combustion of intercalated anions.

The thermal stability of the porphyrin molecules intercalated between the hydroxide layers was investigated by TG-DTA in conjunction with mass spectroscopy. Pure porphyrins and their intercalated phases exhibit complex thermal behavior (Supporting Information Figures S2−S5); therefore, the most sensitive measure of thermal behavior appears to be the evolution of gases due to porphyrin decomposition, namely SO_2 and NO_2. While the onset of the evolution of NO_2 is not affected by intercalation, the evolution of SO_2 starts at lower temperature for both pure porphyrins. Thus, ZnTPPS starts to decompose at ca. 340 °C and the onset is shifted to nearly 465 °C after intercalation. In the case of the Mg_2Al LDH hybrid, the onset is shifted from ca. 310 to 480 °C. These results indicate that host−guest interactions thermally stabilize the porphyrin molecules similarly to other intercalated molecules.[45−47]

XRD Analysis. $Zn_2Al-ZnTPPS^H$ displays very narrow 003n diffraction lines which are characteristic of high coherency materials and a large number of the 10n and 01n in-plane diffraction lines. The latter observation is

(44) Britto, S.; Radha, A. V.; Ravishankar, N.; Kamath, P. V. *Solid State Sci.* **2007**, *9*, 279.
(45) Vaysse, C.; Guerlou-Demourgues, L.; Demourgues, A.; Delmas, C. *J. Sol. State Chem.* **2002**, *167*, 59.
(46) Zhang, X.; Wei, M.; Pu, M.; Li, X.; Chen, H.; Evans, D. G.; Duan, X. *J. Sol. State Chem.* **2005**, *178*, 2701.
(47) Wang, Z.-L.; Kang, Z.-H.; Wang, E.-B.; Su, Z.-M.; Xu, L. *Inorg. Chem.* **2006**, *45*, 4364.

Table 2. Thermogravimetric Data of Porphyrin−LDH Hybrids

samples	weight loss/% < 150 °C	150−400 °C	400−800 °C	nH_2O physisorbed	nH_2O interlayer
Mg_2Al−TPPS	2.6	8	19.1	1.89	0.61
Mg_2Al−$TPPS^H$	6.1	11.3	26.5	2.32	1.48
Zn_2Al−TPPS	5.6	10.2	27	1.33	1.67
Zn_2Al−(Zn)$TPPS^H$	6.2	10.2	22.7	1.13	1.87
Zn_4Al−TPPS	5.7	10.6	22.4	[a]	[a]
Zn_4Al−(Zn)$TPPS^H$	6.1	10.3	23.1	[a]	[a]

[a] Not determined because of the formation of ZnO.

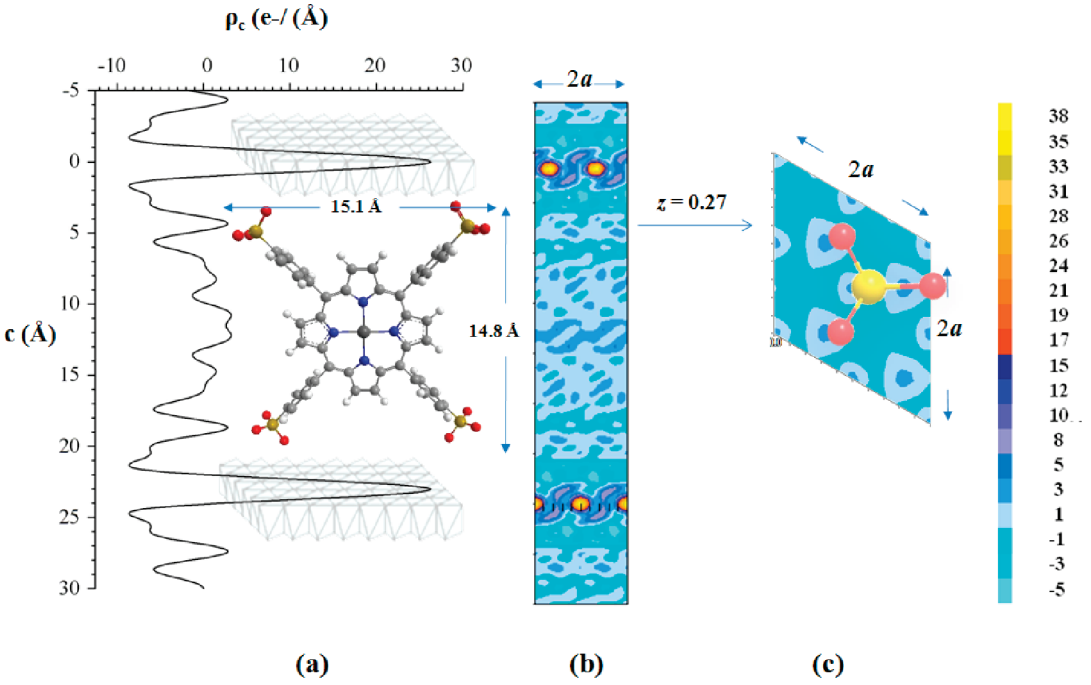

Figure 7. Structure model of Zn_2Al−$ZnTPPS^H$: (a) one-dimensional electron density determined from the Debye−Scherrer data projected along the *c*-stacking axis; (b) contoured Fourier map of the (*x*0*z*) plane (summed from 0 to 1 along the *b*-axis); (c) contoured Fourier map of the (*xy*0) plane ($z = 0.27$). The sulfonate group is overlaid on the (*xy*0) plane to show the matching with the density spots observed at $z = 0.27$ (and $z = 0.07$). The electron density scale (e^-/Å) is given on the right.

quite rare in LDH-based materials because these materials are known to be low crystalline, especially hybrid LDH, due to anisotropic size effects (i.e., platelet morphology), microstrains, and stacking faults. Besides, owing to the small difference between the Zn^{2+} and Al^{3+} X-ray atomic scattering factors and the low contribution expected from light atoms such as C, O, N, S, and H forming the skeleton of the porphyrin guest molecule, it would be too tentative to attribute the in-plane diffraction lines to either a cation ordering of Zn^{2+} and Al^{3+} within the hydroxide layer or to an ordering of the porphyrin molecules in the interlayer space. As the in-plane diffraction lines are expected for a 3R polytype without stacking faults, we can reasonably assume a nearly perfect 3R stacking of the hydroxide layers. It may be attributed to the rigidity of the porphyrin framework.

The large number of 003n diffraction lines (up to seven harmonics) related to the large size of the intercalated porphyrin molecule allows probing the structure of the interlayer space projected on the *c*-axis via the Fourier transformation.[48] The one-dimensional (1D) electron density map for Zn_2Al−$ZnTPPS^H$, determined from Debye−Scherrer data, can be calculated using the known structure of a hydroxide layer, assuming a weak contribution from the interlayer part to total scattering (Figure 7a). The corresponding plots for Mg_2Al−$TPPS^H$ and Zn_2Al−$ZnTPPS^H$ determined using the Bragg−Brentano XRD data are compared in Supporting Information Figure S6A. The difference between the 1D plots for Zn_2Al−$ZnTPPS^H$ displayed in Figures 7a and S6A is due to resolution differences between the two XRD data sets; the high-resolution data obtained in the Debye−Scherrer mode gives the 1D plot with a better resolution.

The 1D electron density map of Zn_2Al−$ZnTPPS^H$ (Figure 7a) displays two strong maxima at 0 and 23 Å corresponding to the metal containing hydroxide layers. The five additional peaks of lower electron densities located in between can be attributed to the intercalated porphyrin and water molecules. Upon comparison with the dimensions of the porphyrin molecule (~ 15/4.3 Å), a

(48) Whittingham, M. S.; Jacobson, A. *Intercalation Chemistry*; Academic Press: New York, 1982.

perpendicular arrangement of the porphyrin plane against the hydroxide layer can be proposed in agreement with previous study.[24] The sulfonate groups cause maxima at the outer parts of the interlayer space at about 4 Å from the center of the hydroxide layers that is consistent with hydrogen bonding interactions between the sulfonate groups and OH groups of the layers. These interactions along with Coulombic interactions dictate the orientation of the anions with respect to the LDH surface.[49] The central maxima and the two peaks on each side arise from the porphyrin ring. The splitting of the central maxima indicates an orientation disorder of the porphyrin molecules around a given central site (see below). If we assumed a perpendicular orientation, the porphyrin molecule would fill a surface area of 16.2 $Å^2/e^-$ that is largely compensated with the surface area of 23.5 $Å^2/e^-$ of the hydroxide layer. A far better accordance could certainly be obtained by slightly inclined molecular planes resulting in an increase of the surface required by the porphyrin molecule. Yet, the present data do not allow distinguishing between a perpendicular and inclined orientation. On the other hand, this result can be compared with the calculation of the interlayer space available for intercalated anions that is often applied in hybrid LDH:[50] 23.03 Å (d_{003}) − 2.10 Å (i.e., hydroxide layer thickness) − 2 × 2.70 Å (i.e., hydrogen bonding) = 15.5 Å. The gallery height thus obtained is comparable with the size of the porphyrin molecule and again indicates a perpendicular or nearly perpendicular orientation of the porphyrin units between the hydroxide layers.

The electron-density distributions on the (*x0z*) and (*xy0*) planes, plotted with the GFourier program,[51] are presented in the form of contour plots in Figure 7b and c. In the same way as for the 1D projection, the phases and structure factors were computed from the known configuration of the hydroxide layer part of the structure. Note that the differences in the electron density between spots in the interlayer space are quite small, preventing us from a detailed description of the interlayer structure. Nevertheless, four important points can be drawn. (i) The highest density peaks observed at $z \sim 0.27$ and 0.07, i.e., 4 Å from the center of the hydroxide layers, are localized vertically to metal cations and can be reasonably assigned to the sulfonate groups. This does not mean that the distance between sulfonate groups is equal to the distance between metal cations within the hydroxide layer, i.e., ~3 Å. Indeed, one must keep in mind that equivalent positions that are too close to one another are only partially occupied by the sulfonate groups, in agreement with the $Zn_2Al-ZnTPPS^H$ chemical formula. The distances around 1.6 Å between density peaks observed at $z \sim 0.27$ (and ~0.07) are consistent with an S−O bond length. (ii) The aromatic ring system gives rise to a rather disordered electron density in the middle of the gallery. Such disorder suggests a low contribution, if any, of a superstructure based on regularly aligned porphyrin units. (iii) Assuming the $R\bar{3}m$ space group, metal ions of two successive hydroxide layers are shifted by 1/3 in the [110] direction, then the sulfonate groups located at the outer parts of the interlayer space exhibit the same shift, leading to a slightly inclined orientation of the porphyrin plane with an angle of ca. 8° with respect to the normal of the hydroxide layer. (iv) The decrease of the electron densities attributed to the sulfonate groups, after a thermal treatment at 100 °C under vacuum, is indicative of the presence of water molecules located nearby the sulfonate groups (Supporting Information Figure S6B).

Comparison of the less resolved one-dimensional plots of $Zn_2Al-ZnTPPS^H$ and $Mg_2Al-TPPS^H$ calculated from the Bragg−Brentano XRD data is valuable since these two samples display the same M^{2+}/M^{3+} molar ratio according to the chemical analysis; hence, they are intercalated with the same amount of porphyrin (Supporting Information Figure S6). The 1D plots show differences in the electron densities at the hydroxide layers and porphyrin ring positions. The lower electron density observed for the Mg_2Al hydroxide layers is due to the difference between Zn ($Z = 30$) and Mg ($Z = 12$) atomic numbers. In addition, the presence of Zn^{2+} in the middle of the porphyrin unit explains the higher electron density in the interlayer central plane of $Zn_2Al-ZnTPPS^H$.

The studies show that ordering of some organic anions within the interlayer galleries is relatively common, in contrast to the generally disordered interlayers filled with inorganic anions.[12] In this respect, we might speculate on the ordering of the porphyrin units. They are bulky and rigid, and the final arrangement is governed by the interplay of the Coulombic interactions of porphyrin anions with the positively charged layers, interactions between neighboring anions, and the hydrogen bonding interactions among the hydroxyl groups, porphyrin sulfonate groups, and water. The indexing calculations either using DiffracPlus Topas (v. 4.1) or Dicvol 2006 give a trigonal cell well-described by $a = 3.0625(3)$ Å, $c = 69.090(1)$ Å, and $\gamma = 120°$. If one assumes that intercalated porphyrin units are ordered and create a superstructure, such an *a* parameter would not allow accommodating the porphyrin molecule with a size of ca. 15 Å. The simplest model that would permit the ordering of ZnTPPS anions within the $R\bar{3}m$ unit cell is the multiple application of the unit cell transformation (IIc, $a' = -2a, b' = -2b$)[52] yielding a new *a* parameter of 24.5 Å. This parameter is comparable with the size of the porphyrin molecule; however, no additional diffraction lines allow this indexing of the XRD patterns. In fact, these additional lines are expected to be very weak, if any, because experimental electron density maps indicate some disorder in the middle of the

(49) Cai, H.; Hillier, A. C.; Franklin, K. R.; Nunn, C. C.; Ward, M. D. *Science* **1994**, *266*, 1551.
(50) Ennadi, A.; Khaldi, M.; de Roy, A.; Besse, J. P. *Mol. Cryst. Liq. Cryst.* **1994**, *244*, 373.
(51) Roisnel, T.; Rodriguez-Carvajal, J. WinPLOTR: a Windows tool for powder diffraction patterns analysis, Materials Science Forum. Proceedings of the Seventh European Powder Diffraction Conference (EPDIC 7), Barcelona, Spain, May 20−23, 2000; Delhez, R., Mittemeijer, E. J., Eds.; Trans Tech Publications Inc.: Switzerland, 2001; p 118−123.
(52) *International Tables for Crystallography*, 5th ed.; Hahn, Th.; Ed.; Springer: Dordrecht, The Netherlands, 2005; Vol. *A*, p 546.

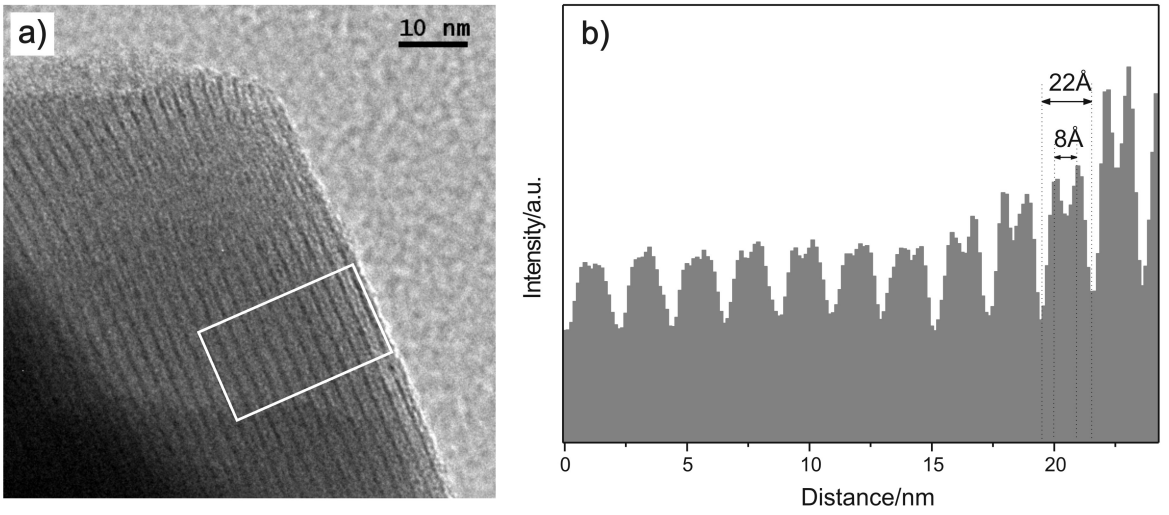

Figure 8. HRTEM observation of $Zn_2Al-ZnTPPS^H$: (a) high-resolution micrograph, (b) intensity histogram of the area marked in part a.

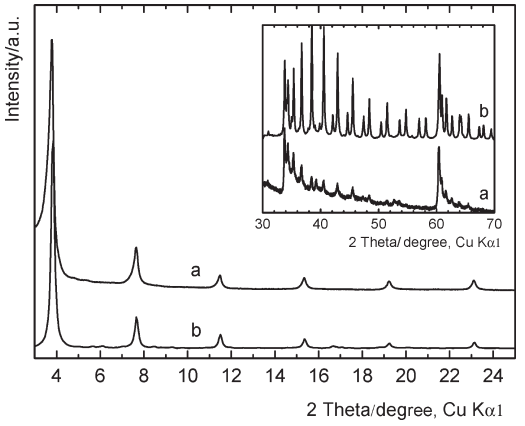

Figure 9. Experimental (a) and calculated (b) XRD basal diffraction lines of $Zn_2Al-ZnTPPS^H$ hybrid. (inset) Corresponding experimental (a) and calculated (b) XRD nonbasal diffraction lines.

interlayer and because of small differences between the atomic scattering factors of hydroxide metals.

Transmission Electron Microscopy. The HRTEM micrographs of original and porphyrin-intercalated LDH were recorded to observe the changes of the layered structure upon intercalation. The particles of original LDH, Zn_2Al-Cl^H, have a typical hexagonal shape; sometimes slightly irregular with the unequal length of sides (Supporting Information Figure S7). The size of the crystals is below 1 μm. The basal spacing of Zn_2Al-Cl^H, measured as a distance between the intensity minima, is about 8 Å (Supporting Information Figure S8), which corresponds to 7.75 Å obtained from the XRD patterns. The distance between the parallel fringes in $Zn_2Al-ZnTPPS^H$ is about 22 Å (Figure 8), which is in good agreement with the d_{003} value of 23.03 Å determined by XRD. Moreover, the HRTEM micrographs reveal additional lattice fringes with a fringe separation of about 8 Å indicating an increase of electron density in the middle of the interlayer space (Figure 8b). In agreement with information obtained from XRD, this suggests that the metal centra of the porphyrin units are aligned in the middle of the interlayer space.

Molecular Modeling. The experimentally accessible XRD patterns bear important structural information. We constructed a structural model using the molecular simulations approach taking the van der Waals dimension of the porphyrin guest and by assuming that the intercalation process does not change measurably the structure of the hydroxide layers. The calculated XRD patterns of the optimized $Zn_2Al-ZnTPPS^H$ structure and the experimental XRD are compared in the 2θ scale in Figure 9. The patterns exhibit typical features of a layered structure, i.e., basal lines 003n. The measured basal spacing (Table 1), line positions, and intensities of diffraction lines are very similar. Some intensity differences might be due to the crystallite morphology and roughness of the sample surface.[53] The calculated XRD has additional very low intensity lines between 5 and 6° and 16 and 18° of the 2θ scale, which appear due to the forced periodicity of the model. In the calculation, the supercell is treated as a structural element, which is infinitely repeated in all directions forming an infinite and perfectly periodic 3D crystal. The forced repeating of the structural elements imposes the periodicity of central zinc atoms of ZnTPPS leading to the appearance of these lines. Indeed, once Zn atoms are removed from the model, the low intensity lines disappear. However, intensities of these diffraction lines are very low and it is difficult to differentiate them from possible imperfections and small amounts of impurities in the real sample.

The observation of the nonbasal lines and their comparison with calculated XRD bring additional information on the layer ordering (Figure 9). The experimental line positions are best reproduced by a model with a = 3.063 and d_{003} = 23.05 Å, the values that correspond well to the experimental ones (Table 1). The higher intensities of some calculated lines are imposed by the perfect layer periodicity of the model. The host layers were kept in the same layer stacking order as in the original nitrate form

(53) Kovář, P.; Pospíšil, M.; Nocchetti, M.; Čapková, P.; Melánová, K. *J. Mol. Model.* **2007**, *13*, 937.

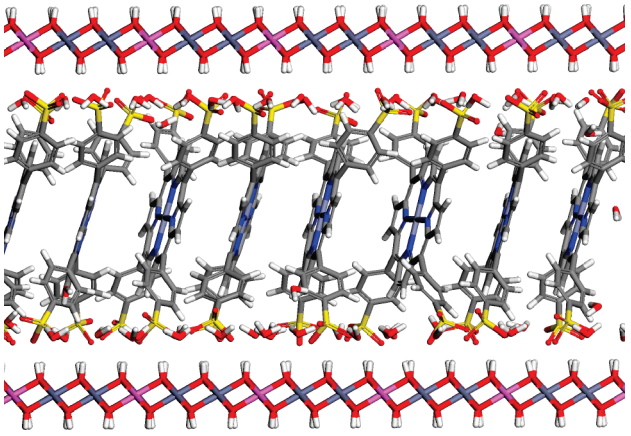

Figure 10. Interlayer space of the Zn_2Al LDH lattice filled with ZnTPPS.

(polytype 3R), therefore, the consistence between the calculated and experimental patterns indicates that the original symmetry is a good approximation for the layer stacking of the investigated intercalate. This is also corroborated by the fact that a horizontal shift of the layers violating the $R\bar{3}m$ symmetry induces many additional diffraction lines in the calculated XRD in disagreement with the experimental diffraction data. Because exchanging the Zn and Al atomic positions within the hydroxide layers does not affect the calculated diffraction patterns, an order/disorder arrangement of Al/Zn atoms is not distinguishable, and the nonbasal diffraction lines are governed only by a translation of atomic positions. Some layer nonperiodicity can be reproduced by the reoptimization of the final model with variable cell parameters (c, α, and β) used in step 2 (see the Supporting Information). It slightly changes the cell angles (0.3° at maximum) with only minor deviations of the layer stacking order, and as a result, the intensities of the calculated and experimental nonbasal diffraction lines are more similar.

The interlayer space in the minimized model (Figure 10) is filled with nearly parallel porphyrin units with a dihedral angle varying between 0 and 10°. The porphyrin planes are not perpendicular to the hydroxide layers. Instead, angle variations between the porphyrin plane and the layer normal satisfy the Gaussian distribution with the average angle of ca. 14° (Supporting Information Figure S9). In agreement with the HRTEM micrographs (Figure 8), porphyrin zinc atoms of ZnTPPS are in the middle of the interlayer space, i.e., 11.525 ± 0.300 Å with respect to the neighboring (003) basal plane (basal spacing is 23.05 Å). Due to a horizontal shift of the porphyrin units, their central Zn atoms are horizontally disordered (Figure 11). The distance between two neighboring porphyrin centra defined as a line connecting Zn atoms varies from 6 to 9 Å. The top view shows that the porphyrin molecules are horizontally shifted by a distance varying from one-third to one-half of the porphyrin size, thus homogeneously occupying the interlayer space (Figure 11). The pyrrole rings of the porphyrin molecule impose a hydrophobic region in the midplane of the interlayer causing that the most of interlayer water molecules are located close to the hydrophilic hydroxide

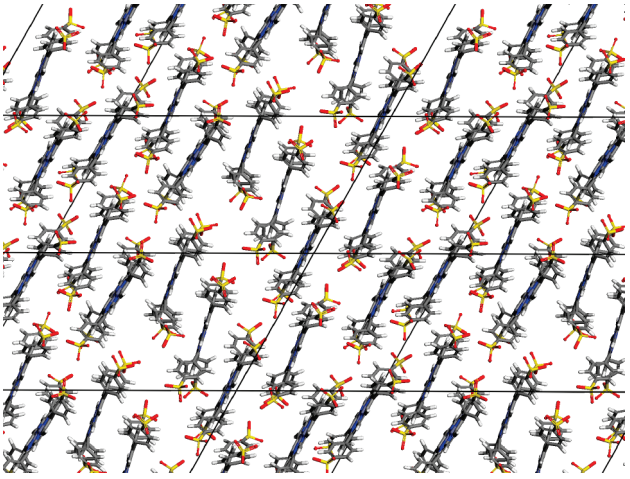

Figure 11. Top view of linked supercells containing ZnTPPS anions in the interlayer space.

layers together with the sulfonate groups of ZnTPPS (Figure 10) as documented by the XRD analysis. In this region, water molecules, oxygen atoms of the sulfonate groups, and the hydroxide surface are in close contacts indicating hydrogen bonding interactions. The hydrogen-bond donor is a surface OH group and the acceptors are oxygen atoms of a water molecule or sulfonate group. Only several water molecules (1−2 molecules per interlayer) are close to porphyrin zinc atoms among the porphyrin units (Figure 10). The modeled structural arrangement documents disorder of the central part of the interlayer that is in agreement with the XRD analysis. The TPPS molecules in the Mg_2Al LDH hosts are aligned similarly; however, the TPPS units can slightly deviate from the planarity.[33]

To complement the model description, the atom concentration profile of the optimized interlayer was compared with the experimental electron density map (Supporting Information Figure S10). The concentration profile is derived from the atomic densities assuming the equivalence of all atoms. While the electron density peaks of the hydroxide layers (d = 0 and 23 Å) and water molecules together with the sulfonate groups ($d \sim 4$ and 19 Å) are well-reproduced by the concentration profile, the concentration of porphyrin zinc atoms in the middle of the interspace is expectantly of very low intensity. The electron density peaks of pyrrole atoms located near 8 and 15 Å are shifted by about 0.8 Å to the middle of the interspace. It might indicate that central zinc atom attracts nitrogen and carbon electrons toward the porphyrin center.

Photophysical Properties. The results document that LDH hosts are well suited for accommodating the porphyrin molecules. The absorption spectra enable the characterization of the molecular state of porphyrins because their aggregation is accompanied by considerable spectral changes. Comparing the absorption spectra of monomeric porphyrin solutions with those of TPPS and ZnTPPS intercalated in LDH, it is evident that the intercalation does not significantly alter the shape of the Soret band but only broadens it, an effect that we assign

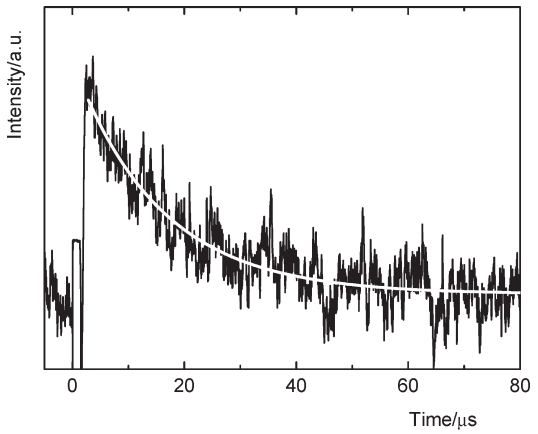

Figure 12. Time dependence of the $^1O_2$ luminescence signal of Mg_2Al−TPPS (λ_{exc} = 425 nm, ~ 1 mJ, oxygen atmosphere, recorded at 1270 nm). The smoothed line is a least-squares monoexponential fit.

to a range of binding sites of the porphyrin molecules. Thus, extensive porphyrin aggregation, a process that often occurs in solutions and on solid templates, is ruled out.[10,54] This is consistent with the molecular modeling results showing that the distance between two neighboring central atoms varies between 6 and 9 Å. The distance is considerably larger than the typical van der Waals separation of about 3.5 Å observed in π stacking of aromatic compounds.

Recently, we have described the photophysical properties of Mg_RAl hybrids containing intercalated porphyrin molecules.[29,30] The production of $O_2(^1\Delta_g)$ was predicted on the basis of quenching of the porphyrins triplet states by molecular oxygen and directly evidenced using time-dependent luminescence spectroscopy at 1270 nm. The same approach was applied here on Zn_RAl and Mg_RAl LDH hybrids prepared by the coprecipitation method. Figure 12 depicts the $O_2(^1\Delta_g)$ luminescence intensity recorded after excitation of Mg_2Al−TPPS hybrid. The effective lifetime of $O_2(^1\Delta_g)$ recovered from the monoexponential fits is 16 μs. Since pure LDH hosts do not exhibit any $O_2(^1\Delta_g)$ luminescence, it is evident that $O_2(^1\Delta_g)$ is generated solely by the porphyrin photosensitized reaction. Surprisingly, the formation of $O_2(^1\Delta_g)$ was observed only for the hybrids based on Mg_RAl LDH hosts practically not depending on the sample crystallinity, while Zn_RAl LDH-based hybrids do not produce any measurable amount of this species. The explanation is not clear because both TPPS and ZnTPPS are effective sensitizers with high quantum yields of $O_2(^1\Delta_g)$ in aqueous solutions.[55] We suppose that the lifetimes of the porphyrin triplet states and $O_2(^1\Delta_g)$ are considerably affected by Zn- and Al-coordinated OH groups oriented toward the interlayer space. Evidently, the best photosensitizing LDH materials studied in this paper are based on the Mg_RAl LDH hosts.

(54) Xu, W.; Guo, H. Q.; Akins, D. L. *J. Phys. Chem. B* **2001**, *105*, 1543.
(55) (a) García-Ortega, H.; Bourdelande, J. L.; Crusats, J.; El-Hachemi, Z.; Ribó, J. M. *J. Phys. Chem. B* **2004**, *108*, 4631. (b) Mosinger, J.; Micka, Z. *J. Photochem. Photobiol. A* **1997**, *107*, 77.

Conclusions

LDH are suitable hosts of porphyrin sensitizers. Porphyrin TPPS is intercalated in Mg_RAl LDH (R = 2−4) to give the hybrids with a characteristic basal spacing of about 23 Å. Similar results are obtained for ZnTPPS within the Zn_RAl LDH interlayer space (R = 2−4). The hydrothermal treatment increases crystallinity of the hybrids and originally intercalated TPPS in Zn_RAl LDH is metalated to ZnTPPS, while intercalated TPPS in Mg_RAl LDH remains unchanged.

The presented results can be summarized as follows. (i) The rigid framework of ZnTPPS has a benefical effect on the ordering of the hydroxide layers. (ii) The diffraction patterns are well characterized by the $R\bar{3}m$ rhombohedral space group, typical of LDH-based systems. (iii) Intercalated porphyrins do not aggregate, which is a prerequisite of effective photosensitization of $O_2(^1\Delta_g)$. The distance between two neighboring central atoms varies from 6 to 9 Å that is much longer than that of about 3.5 Å typical in parallel stacking of aromatic compounds. (iv) The gallery height of 15.5 Å is filled with nearly parallel porphyrin units. The porphyrin units are inclined with respect to the hydroxide layers with the average angle between the porphyrin plane and the layer normal of about 14°. Central zinc atoms of ZnTPPS are in the middle of the interlayer space. (v) The sulfonate groups are about 4 Å from the center of the hydroxide layers indicating the hydrogen bonding interactions between the sulfonate groups and OH groups of the layers with the contribution of water molecules. (vi) The disorder in the middle of the gallery suggests a low contribution, if any, of a superstructure based on regularly aligned porphyrin units. (vii) Mg_RAl−TPPS hybrids produce $O_2(^1\Delta_g)$, while no measurable amount of this species was found for Zn_RAl LDH-based hybrids.

Acknowledgment. This work was supported by the Czech Science Foundation (Nos. P207/10/1447, 203/07/1424), the Ministry of Education, Youth and Sports of the Czech Republic (Nos. MSM 0021620835, MSM 0021620857), and the French National Center of Scientific Research CNRS (No. 22538). The authors thank Zdeněk Futera (Faculty of Mathematics and Physics, Charles University in Prague) for ab initio calculations of the ZnTPPS porphyrin geometry.

Supporting Information Available: Details of characterization techniques and molecular modeling; TG-DTA curves, one-dimensional electron densities; HRTEM micrographs; angle distributions; experimental electron density vs atom concentration profiles. This material is available free of charge via the Internet at http://pubs.acs.org/.